RSC Advances

ROYAL SOCIETY OF CHEMISTRY

www.rsc.org/advances

The multi-channel reaction of OH radical with 5-hydroxymethylcytosine: a computational study

Lingxia Jin[*,a] Caibin Zhao[a] Cunfang Liu[a] Suotian Min[a]

Tianlei Zhang[a] Zhiyin Wang[a] Wenliang Wang[*,b] Qiang Zhang[a]

[a]*Shaanxi Province Key Laboratory of Catalytic Fundamentals & Applications, Shaanxi Key Laboratory for Resource Biology, Vitamin D Research Institute, School of Chemical & Environment Science, Shaanxi University of Technology, Hanzhong 723001*

[b]*Key Laboratory for Macromolecular Science of Shaanxi Province, School of Chemistry and Chemical Engineering, Shaanxi Normal University, Xi'an 710062*

Abstract

Hydroxyl radical may attack on the new cytosine derivative (5-hydroxymethylcytosine, 5-hmCyt) causing DNA oxidative damage, whereas the study of the related mechanism is still in its infancy. In the present work, two distinct mechanisms have been explored by means of CBS-QB3 and CBS-QB3/PCM methods, the addition of •OH to the nucleophilic C5 (R1) and C6 (R2) atoms and the H-abstractions from the N4 (R3 and R4), C7 (R5 and R6), C6 (R7) and O3 (R8) atoms of 5-hmCyt, respectively. The solvent effects of water do not significantly alter the energetics of the addition and abstraction paths compared to those in the gas phase. The •OH addition to C5 and C6 sites of 5-hmCyt are energetically more favorable than to N3, C4 or O2 sites, and the $\Delta G^{s\neq}$ value of C5 channel is a little lower than that of C6 route, indicating some amount of regioselectivity, which is in agreement with the conclusions of •OH-mediated cytosine reaction reported by experimentally and theoretically. The H5 and H6 abstraction reactions are more favorable than other abstractions, which have almost the same energy barriers as those of •OH addition to C5 and C6 sites. Moreover, the energies of the H5 and H6 dehydrogenation

* Corresponding authors: Tel: +86-916-2641660; e-mail: jinlingxia1982@126.com (L.X. Jin); Tel: +86-29-81530815 Fax: +86-29-81530727; e-mail: wlwang@snnu.edu.cn (W. L. Wang).

†Electronic supplementary information (ESI) available: The relevant information of different 5-hmCyt tautomers and their isomerization reactions both in the gas and aqueous phases are shown in Table S1. The energy information for the addition of •OH to C2, N3 and C4 sites of 5-hmCyt both in the gas and aqueous phases are listed in Table S2. The energy profiles along the dihedral angle O3C7C5C4 in 5-hmCyt and optimized structures of 5-hmCyt tautomers and the isomerization transition states are shown in Figs.S1 and S2. The minimum energy paths of paths R5 and R6 are given in Figs.S3 and S4. The important bond lengths of all stationary points of the main addition and hydrogen abstraction paths in the aqueous phase are listed in Figs.S5-S7.

products formed benzyl-radical-like complex, are about 62~101 kJ·mol^{-1} higher than those of the adduct radicals, indicating that the H5 and H6 abstractions have a relatively high probability to happen. And by that analogy, the proportion of the H5 and H6 dehydrogenation products are large and may be detectable experimentally. These hint that the new DNA base (5-hmCyt) is easily damaged when exposed the surrounding of hydroxyl radicals environment. Therefore the reducing free radical production or the addition of some antioxidants should be taken in mammalian brain tissues to resistance DNA damage. Our results provide some evidences between 5-hmCyt and tumor development for the experimental scientists.

1. Introduction

DNA contains the complex hereditary information within the cells of living organisms. Organisms must keep the integrity of their DNA aimed to remain healthy and propagate. Both normal metabolic activities, and environmental effects can damage DNA.[1-11] When damage accumulates to the extent that it can no longer be repaired, some major problems may occur. These are senescence, programmed cell death, and carcinogenesis, and are manifested by aging, neurological syndromes, and cancer. Thus, the identification and repair of DNA damage are an important factor in improving human health and longevity. The tremendous attentions have focused on the causes of DNA damage, both exogenously and endogenously. One of them is oxidative damage of cellular DNA by free radicals, which may be a significant factor in human carcinogenesis.[12-16] The appropriate amount of radicals may have a great effect on the immune response, cell differentiation, apoptosis and the processes of biochemical metabolism, whereas the excessive radicals will be an oxidation press to the organism, which cause serious destruction to the biological macromolecules.[17,18] The hydroxyl radical (•OH) is an important reactive oxygen species (ROS), and appears to be the most damaging.[13,19,20] Normally, •OH is usually present at very low levels in biological systems, mainly arising from the exposure of cells to exogenous chemical and physical agents. In general, OH radicals modify the DNA through either hydrogen atom abstraction or hydroxyl radical adduction, which leads to sugar and base modifications that threaten genomic integrity due to their mutagenic potential.[21,22]

Approximately half of the damage caused by OH radicals occurs on nucleobases. 5-hydroxymethylcytosine (5-hmCyt) is the oxidative product of nucleobase (5-methylcytosine), at

surprisingly high abundance in mammal brain and embryonic stem cells.[23-26] It has recently discovered as a new constituent of mammalian DNA, which is considered to be the sixth base of the genome of higher organisms. [23-26] It might serve unique biological roles in many biological processes such as gene control mechanisms, DNA methylation regulation, and involved in many diseases, especially cancers. The level of 5-hmCyt in cancer is significantly reduced and changed in different types of tumor, which shows that it may play a role in tumorigenesis and development process. However, the exploration of the relationship between 5-hmCyt and tumor development is still in the initial stage. [27] Additionally, it is well known[28] that oxidative damage of DNA bases by hydroxyl radical are the focus of the development for certain cancers, stimulating a lot of interest in whether the reactivity of •OH with new nucleoside is similar as compared to those of the four DNA nucleobases. Thus like the four DNA nucleobases, •OH typically adds to the double bonds of nucleobases to yield adducts radicals, and directly abstracts hydrogen to produce dehydrogenated radicals, respectively. Even though the reaction of the •OH with 5-hmCyt is essentially lacking in experiment and theoretically, it is important to study all the ways in which free radicals can cause oxidative DNA damage.

As mentioned above, the addition and abstraction reactions for •OH with 5-hmCyt will be performed a detailed computational study. Then, two aspects are concerned as follows: firstly, the difference of the free energy barriers between the addition and H-atom abstraction reaction in the process of •OH-mediated 5-hmCyt are explored from a theoretical perspective to clarify whether the addition can kinetically compete with their abstraction; meanwhile, the solvent effect on reaction mechanisms and activation free energies are examined. Our calculations point out the corresponding reaction pathways and energetics, which may be the theoretical aid for the experimental scientists for further understanding the formation of tumor.

2. Computational methods

All the calculations were performed using the Gaussian 09 package.[29] From our previous work, it has been found that the activation free energies calculated using CBS-QB3[30] and G3B3 [31]approaches agree well with each other, proving that these two approaches are able to provide reliable data for our system. However, the G3B3 composite approach is relatively computationally expensive. Moreover, the previous studies have shown that the CBS-QB3 method can provides adequately accurate energies, with a standard deviation of about 1.5 kcal•mol^{-1}.[32-34]

Thus the single point energies of the species have been refined at the CBS-QB3 level of theory. Specifically, the composite CBS-QB3 method, using CBSB4 for its MP4SDQ calculation and CBSB3 for the MP2 calculation, is widely used to obtain accurate energies of molecules. Besides, this approach includes empirical corrections for spin contamination.[30, 35-40]

The CBSB7 method was applied to the gas phase calculations and additionally the polarizable continuum model (PCM)[41] with dielectric constant 78.39 of the solvent for the aqueous solution. Frequency analysis has also been computed at the same level of theory to verify whether the obtained structures are transition structures or local minima. Intrinsic reaction coordinate (IRC)[42] calculations have been carried out from each transition state to ensure that the obtained transition state connected the appropriate reactants and products.

3. Results and discussion

3.1 Stationary point structures and energetics in the gas phase

The potential energy based on the torsion and the angle of the OH group in 5-hmCyt is depicted in Fig. S1. There are the four energy minimum and three maximum points. These minimum and maximum points are optimized by CBS-QB3 method (Fig. S2). The energy minimum points are corresponding to three isomers (M1, M2, and M3) with all real frequencies. The energy maximum points are three transition states TSM1/M2, TSM2/M3 and M3/M1 with only one imaginary frequency (the values are 91.87 *i*, 153.84 *i* and 91.87 *i* cm^{-1}, respectively). And two of them (M2 and M3) are mirror image isomerism. The order of stability obtained in the aqueous phase is M3=M2>M1, suggesting M3 (M2) is a little more stable than M1 (Table S1). Thus on the basis of this result, the more stable M3 isomer has been chosen for the present computational study.

3.1.1 Addition reaction mechanism of •OH with 5-hmCyt

The structural features of 5-hmCyt are favored C2, O2, N3, C4, C5 and C6 as the addition sites. The constituent atoms are expected to be more reactive for the electrophilic addition reaction with hydroxyl radical. However, as for the O2 site, various initial geometries of adducts have been designed, but the •OH is always far from O2 atom. Thus the addition of •OH to these atoms (C2, N3, C4, C5 and C6) of 5-hmCyt are investigated both in the gas and aqueous phases (Tables S2 and 1). As seen from Tables S2 and 1, it is obviously shown that the energy barriers for the addition of the •OH at the different atoms follow the order C5 < C6 < C4 < C2 < N3, the

difference between the energy barriers corresponding to the C5 and N3 sites being 66.60 kJ·mol^{-1}. The relative stabilities of the different adducts is C6 < C5 < C4 < C2 < N3. Moreover, the addition of •OH to C2, N3 and C4 sites both in the gas and aqueous phases are highly endothermic with respect to their energies of the reaction complexes, whereas the reactions of C5 and C6 sites are exothermic relevant to their energies of the reaction intermediates. These results imply that the addition of •OH to the C5 and C6 sites for 5-hmCyt are both thermodynamically and kinetically more favorable than to other sites, which would be most probable to happen in experiments. Thus the reactions of •OH at the C5 and C6 sites of 5-hmCyt have been further explored in detail.

The •OH addition occurs when the oxygen of the •OH approaches the π-face of the 5-hmCyt to form the reaction complex IM1. Due to this interaction, the bond length of C5=C6 (1.358 Å) in 5-hmCyt is activated to 1.378 Å in IM1 and paves the way for a facile addition reaction. Two addition pathways are observed from IM1, one leading to the adduct 5-hmCyt-C5OH• (P1) via transition state TS1 and the other to the adduct 5-hmCyt-C6OH• (P2) via TS2 (Fig. 1).

As seen from in Table 1, the activation free energy ($\Delta G^{g\neq}$) for the first addition pathway (R1) is 0.20 kJ·mol^{-1} while the $\Delta G^{g\neq}$ value of the second addition pathway (R2) is 5.81 kJ·mol^{-1}, which means that both the reactions are nearly barrierless. The adduct 5-hmCyt-C6OH• (P2) is thermodynamically 28.30 kJ·mol^{-1} more stable than 5-hmCyt-C5OH• (P1). This result indicates that the OH• addition to C6 site is thermodynamically more favorable than to C5 site. However, there is a little small energy barrier (5.81 kJ·mol^{-1}) for the •OH addition to C6 site, while there is nearly barrierless (0.20 kJ·mol^{-1}) for addition to C5 site. This implies that the •OH addition to C5 site is a little more kinetically favorable than to C6 site. Thus though both the reactions are nearly barrierless, the observed small difference in the activation energy barriers indicates some amount of regioselectivity. As seen form Table 2 and Fig. 2, during the formation of the π-complex, significant amount of the spin density from the O of the •OH is transferred to the ring carbon atom and the spin distribution changes on the ring carbon site is further enhanced in the transition state as well, suggesting strong coupling between the π and the unpaired electron densities.

3.1.2 H-abstraction reaction of •OH with 5-hmCyt

The •OH is abstracting from the H3 and H4 of NH_2 group, the H5 and H6 of C7 atom, the H7 of cyclic C6 and H8 of O3 atoms for 5-hmCyt, denoted as paths R3~R8, respectively. Noted that the abstractable H6 and H7 atoms are located closer to the •OH group leading to the formation of

these π-boned complexes. More interestingly, the same π-boned complex is obtained as compared with IM1 by the corresponding IRC calculation. Thus these π-boned complexes are denoted as IM1 in the following discussion.

The H-abstractions from the N4 atom can take place when the reactant complexes IM3 and IM4 are firstly formed (Fig. 3). IM3 will lead to the formation of H3 dehydrogenation products whereas IM4 will account for the H4 abstraction. Compared to the infinitely separated 5-hmCyt and •OH, the IM3 is stable by 36.78 kJ·mol^{-1} and IM4 is only stable by 0.56 kJ·mol^{-1}. In IM3, the distances of H3···O1 and H1···N3 are 2.090 Å and 1.878, respectively, while in IM4, the distances of H4···O1 and H8···O1 are 2.274 Å and 1.880, respectively. Both distance parameters and combined with the stereo-hindrance effect suggest that the stability of IM4 is a little worse than IM3. Interestingly, as seen from Fig. 3, the TS3 is formed six-centered structure, while transition state TS4 is expanded to eight-centered structure and the steric strain is eased. This leads to the $\Delta G^{g\neq}$ value for the abstractable H4 obviously reduced to 9.98 kJ·mol^{-1}, which amounts to a decrease by about 38 kJ·mol^{-1} relative to that for abstraction from H3 atom. Additionally, the product P4 from TS4 is 47.34 kJ·mol^{-1} more stable than the product P3 from TS3. It means that the abstraction of H3 is a little endothermic with respect to the energy of IM3 and the H4 is a slightly exothermic relative to the energy of IM4. The $\Delta G^{g\neq}$ values for the formation of the products P3 and P4 are 48.23 and 9.98 kJ·mol^{-1}, respectively. Thus the gas phase calculations clearly demonstrate that the H4 abstraction is highly favored due to kinetic and thermodynamic control while the H3 abstraction can only results from weak kinetic factors.

The H-abstractions from the C7 atom can take place when the H-bonded complex IM5 and the π-boned complex IM1 are formed, leading to the formation of the corresponding transition states TS5 and TS6 (Fig.4). As for the TS5, the H5 abstraction occurs at the O1···H5 distance of 2.520 Å and the H5···C7 distance of 1.103 Å, which is lengthened by about 3.6% of the original H5-C7 bond length in 5-hmCyt. The transition state for H6 abstraction from C7 occurs later, when the O1···H6 distance is 2.244 Å. Even though O1 is always far away from the abstractable atoms in TS5 and TS6, the H5 and H6 can still be abstracted (Figs.S3 and S4). The $\Delta G^{g\neq}$ value of the H6 abstraction reaction, relative to that of the H5 abstraction, is 10.28 kJ·mol^{-1}. The H5 and H6 abstractions both are highly strong exothermic reactions, which result from the formation of benzyl-radical-like products (P5 and P6), and the product P5 is 10.23 kJ·mol^{-1} more stable than the

product P6. This suggests that relative to that of the H6 abstraction, the abstraction H5 is more favored both thermodynamic and kinetic factors.

The H-abstractions from the C6 and O3 atoms occur from the reactant complexes IM1 and IM8 (Fig. 5). Starting from the H-bonded complexes, the abstractable H7 and H8 atoms are located closer to the •OH group associated with $\Delta G^{g\neq}$ values of 36.27 and 36.11 kJ·mol^{-1}, respectively. Eventually, the H_2O will be eliminated to yield the corresponding product radicals (P7 and P8). As seen from Table 1 and Fig. 6, two paths are thermodynamically and kinetically favorable.

Above all, the activation free energy of the reaction (R5) is small and the formation of product radical is quite stable, which is the most favored both thermodynamic and kinetic factors among all the hydrogen abstractions of 5-hmCyt by OH radical.

As seen form Table 2 and Figs. 2 and 7, it may be noted that unlike the π-complex IM1, the other abstractable complexes (IM3, IM5 and IM8) are the hydrogen bonded complexes, showing only little change among them in the spin density on the O of the •OH except for IM4. As for IM4, besides the formation of a doubly hydrogen bonded complex, the distance of O1⋯N4 is 2.337 Å formed π-boned complex, which leads the spin density from the O of the •OH transferred to the N4 atom. On the other hand, in the corresponding transition states beyond TS5, the spin densities on the O of the •OH variations are drastically even more than the addition transition states TS1 and TS2. And one reason is that there is almost no difference in structures of the reactant complex (IM5) and transition state (TS5), which causes almost no change in the spin density on the O of the •OH (Figs. 7 and S3).

From the above, the energy barriers of the •OH addition to both the C5 and C6 positions for 5-hmCyt is less than 5.81 kJ·mol^{-1} while the H5-abstraction from the C7 site is 5.32 kJ·mol^{-1}, which are nearly barrierless. Meanwhile, the dehydrogenation product radicals are quite stable, suggesting that this reaction has more reaction probability according to the present result. Besides, the H4 and H6 abstractions might be competitive with the above reactions, having $\Delta G^{g\neq}$ values of 9.98 and 15.60 kJ·mol^{-1}, respectively, which are only 4-15 kJ·mol^{-1} more energetic than the results for the most favored reactions. Then, it is of great curious whether the $\Delta G^{g\neq}$ values of these paths will be influenced by the contribution of the bulk water.

3.2 Stationary point structures and energetics in the aqueous phase

The effect of solvation is taken into account using CBS-QB3/PCM method, and it is observed that the solvation has no significant effect on the relative energies of the addition and abstraction reactions. As seen from Figs. S5-S7, the reactant complexes, transition states and products in the aqueous phase show slightly difference when compared to the gas phase results, implying that the small geometrical changes are induced by the presence of the bulk water. As seen from Table 1, the tendency of energy variations for the •OH addition in the aqueous phase is nearly the same as that of the gas phase calculations. The influence of solvation on the activation free energies can be explained by the evolution of the dipole moments for all paths (Table 3).

For the addition reactions at the C5 and C6 positions, the dipole moments of TS1 and TS2, relative to IM1, have very small change by about 0.2 debye, indicating that water has no significant effect on paths R1 and R2. Identify with paths R1 and R2, for the H7-abstraction reaction (R7), solvation is also comparatively negligible. For the other abstraction reactions (R3, R4, R5 and R8), the dipole moments (u=8.30 debye for TS3, u=4.00 debye for TS4, u=5.24 debye for TS5, and u=5.36 debye for TS8) are smaller than their reactant complexes (u=8.73 debye for IM3, u=4.07 debye for IM4, u=5.95 debye for IM5 and u=8.31 debye for IM8), and then the solvent water destabilizes the transition states. This can explain why the steps of these paths are associated with the higher free energy barriers in the aqueous phase than in the gas phase. On the contrary, the dipole moment of TS6 (u=6.28 debye) is more than that of IM1 (u=5.68 debye), and then the solvation of water on TS6 is stronger than that on IM1, leading to an decrease of free energy barrier by 10.86 kJ·mol^{-1} as compared to that in the gas phase.

From Table 1, the $\Delta G^{s\neq}$ values of these paths in the aqueous phase are 0.24, 5.14, 56.96, 19.71, 12.00, 4.74, 38.52 and 44.86 kJ·mol^{-1}, respectively. It is obviously that for the addition, 5-hmCyt shows nearly barrierless for the C5 channel and a small barrier of 5.14 kJ·mol^{-1} for the C6 route. As for the abstraction reactions, the H5 and H6 are the most favorable to be abstracted than other hydrogen atoms. There may be a competitive reaction between the favored addition and abstraction.

4. Summary and conclusions

Two distinct mechanisms are considered by means of CBS-QB3 and CBS-QB3/PCM methods, the addition of •OH to the nucleophilic C5 and C6 atoms and the H-abstractions from the N4, C6, C7 and O3 atoms of 5-hmCyt, respectively. Use of implicit solvent models (PCM) does

not significantly alter the energetics of the addition and abstraction paths compared to those in the gas phase. In the aqueous phase, the $\Delta G^{s\neq}$ values of these paths are 0.24, 5.14, 56.96, 19.71, 12.00, 4.74, 38.52 and 44.86 kJ·mol^{-1}, respectively. The •OH addition to C5 and C6 sites of 5-hmCyt is energetically more favorable than to C4, N3 or O2 sites, and the $\Delta G^{s\neq}$ value of C5 channel is a little lower than that of C6 route, indicating some amount of regioselectivity, which is in agreement with the conclusions of •OH-mediated cytosine reaction reported by experimentally[43] and theoretically.[21(h)] In the six hydrogen-atom abstractions of 5-hmCyt by •OH, the H5 and H6 abstractions are more favorable. These hydrogen-atom abstractions have almost the same energy barriers as those of •OH addition to C5 and C6 sites. Moreover, the energies of the H5 and H6 dehydrogenation products formed benzyl-radical-like complexes, are about 62~101 kJ·mol^{-1} higher than that of the adduct radicals. This implies that H5 and H6 abstractions might be competitive with the additions, having $\Delta G^{s\neq}$ values of 12.00 and 4.74 kJ·mol^{-1}, respectively, which are only 0.40-11.76 kJ·mol^{-1} more energetic than for the addition reactions. In comparison with the •OH addition to C5 and C6 sites of 5-hmCyt, the H5 and H6 abstractions have also more reaction probability. Therefore the proportions of the H5 and H6 dehydrogenation products are large and may be detectable in experiments. As far as we know, this is firstly theoretical report unveiling the reactivity of new nucleoside with •OH, which is also likely to be a little help for the study of the possible mechanisms in tumorigenesis.

5. Final remarks

Our computed results have verified the •OH addition to the C5 and C6 sites as well as H5 and H6 abstraction reactions are both thermodynamically and kinetically more favorable than other sites. These hydrogen abstraction reactions have almost the same energy barriers as those of •OH addition to C5 and C6 sites and the products are quite stable. Hence, these reactions are also likely to happen according to the present results, hinting that the DNA bases are easily damaged when exposed the surrounding of hydroxyl radicals environment. These radicals may capture electrons forming closed-shell anions, or may protonate and restore the original DNA component, or undergo nucleobase loss and other damaging consequences. The DNA bases are easy to be damaged due to the quite lower free barriers of •OH with 5-hmCyt, making the cellular DNA much more likely that cancer will result. Conversely, the exorbitant stability of the adduct/dehydrogenated radicals disfavor to the repair of DNA bases. Therefore, some protective

measures for DNA bases should be taken. For example, some antioxidants should be added in mammalian brain tissues. The reason is that the many antioxidants that can protect biomolecules against DNA damage. However, antioxidant protection against free radicals should be taken with caution since the antioxidant action might actually stimulate cancer progression through the enhanced survival of tumour cells. Of course it would be better to avoid all the radicals for DNA bases. This work might provide some implications for clarifying the reason of these diseases caused by •OH mediated damage to biomolecules.

Acknowledgment

This work was supported by the Shaanxi Province Education Ministry Research Foundation (16JK1153), Brainstorm Project on Social Development by Department of Science and Technology of Shaanxi Province (2015SF270), Shaanxi Province Natural Science Foundation Research Project (2014JQ3109), National Natural Science Foundation of China (No: 31402071, 21473108, 21502109), Shaanxi Innovative Team of Key Science and Technology (2013KCT-17), and the introducing talents Foundation of Shaanxi University of Technology (No: SLGQD14-10, SLGKYQD2-13).

References

1 D. K. Hazra and S. Steenken, *J. Am. Chem. Soc*., 1983, **105**, 4380-4386.
2 S. Steenken and S. V. Jovanovic, *J. Am. Chem. Soc*., 1997, **119**, 617-618.
3 S. D. Wetmore, R. J. Boyd and L. A. Eriksson, *J. Phys. Chem. B*, 1998, **102**,10602-10614.
4 L. P. Candeias and S. Steenken, *Chem. -Eur. J*., 2000, **6**, 475-484.
5 S. S. Wallace, *Free Radical Biol*. Med., 2002, **33**, 1-14.
6 M. Krauss and R. Osman, *J. Phys. Chem. A*, 1997, **101**, 4117-4120.
7 C. J. Mundy, M. E. Colvin and A. A. Quong, *J. Phys. Chem. A*, 2002, **106**, 10063-10071.
8 Y. Wu, C. J. Mundy, M. E. Colvin and R. Car, *J. Phys. Chem. A*, 2004, **108**, 2922-2929.
9 M. H. Almatarneh, C. G. Flinn and R. A. Poirier, *J. Chem. Inf. Model.*, 2008, **48**, 831-843.
10 R. H. D. Lyngdoh and H. F. Schaefer, *Acc. Chem. Res*., 2009, **42**, 563-572.
11 A. Kumar and M. D. Sevilla, *Chem. Rev*., 2010, **110**, 7002-7023.
12 B. Halliwell and O. I. Aruoma, *DNA and Free Radicals*, Ellis Horwood, New York, 6th edn, 1993.
13 C. Von Sonntag, *The chemical basis of radiation biology*, Taylor & Francis, London, 1987.
14 M. Dizdaroglu, *Free Radic. Biol. Med*., 1991, **10**, 225-242.
15 P. Herait, G. Ganem, M. Lipinski, C. Carlu and C. Micheau, *Br. J. Cancer*, 1987, **55**, 135-139.
16 B. Halliwell and J. M. C. Gutteridge, *Free radicals in biology and medicine*, Clarendon, Oxford, 1989.
17 T. Finkel and N. J. Holbrook, *Nature*, 2000, **408**, 239-247.
18 B. N. Ames, M. K. Shigenaga and T. M. Hagen, *Proc. Natl. Acad. Sci. U. S. A.*, 1993, **90**, 7915-7922.
19 A. J. Bertinchamps, J. Hüttermann, W. Köhnlein and R. Teoule, *Effects of ionizing radiation on DNA*, Springer, Berlin, 1978.

20 W. A. Bernhard, *Adv. Radiat. Biol*., 1981, **9**, 199-280.

21 (a) C. J. Burrows and J. G. Muller, *Chem. Rev*., 1998, **98**, 1109-1152; (b) J. Cadet, M. Berger, T. Douki and J. L. Ravanat, *Rev. Physiol. Biochem. Pharmacol*., 1997, **131**, 1-87; (c) W. K. Pogozelski and T. D. Tullius, *Chem. Rev*., 1998, **98**, 1089-1108; (d) J. R. Wagner, C. Decarroz, M. Berger and J. Cadet, *J. Am. Chem. Soc*., 1999, **121**, 4101-4110; (e) J. Cadet, T. Douki and J. L. Ravanat, *Acc. Chem. Res*., 2008, **41**, 1075-1083; (f) G. Pratviel and B. Meunier, *Chem. -Eur. J*., 2006, **12**, 6018-6030; (g) J. R. Wagner and J. Cadet, *Acc. Chem. Res*., 2010, **43**, 564-571; (h) Y. J. Ji and Y.Y. Xia, *Int. J.Quantum Chem.*, 2005, **101**, 211-218; (i) F. M. Antonio, M. Manuela and R. S. Daniel, *J. Phys. Chem. B*, 2014, **118**, 2932-2939; (l) A. Adhikary, A. Kumar, A. N. Heizer, B. J. Palmer, V. Pottiboyina, Y. Liang, S. F. Wnuk and M. D. Sevilla, *J. Am. Chem. Soc*., 2013, **135**, 3121-3135.

22 (a) J. Cadet, T. Delatour, T. Douki, D. Gasparutto, J. P. Pouget, J. L. Ravanat and S. Sauvaigo, *Mutat. Res*., 1999, **424**, 9-21; (b) C. Chatgilialoglu, M. D. Angelantonio, M. Guerra, P. Kaloudis and Q. G. Mulazzani, *Angew. Chem*., 2009, **48**, 2214-2217.

23 Z. Y. Sun, J. Terragni, J. G. Borgaro, Y. W. Liu, L. Yu, S. X. Guan, H. Wang, D. P. Sun, X. D. Cheng, Z. Y. Zhu, S. Pradhan, Y. Zheng, *Cell Rep*., 2013, **3**, 567-576.

24 J. M. Freudenberg, S. Ghosh, B. L. Lackford, S. Yellaboina, X. F. Zheng, R. F. Li, S. Cuddapah, P. A. Wade, G. Hu and R. Jothi, *Nucl. Acids Res*., 2012, **40**, 3364-3377.

25 O. Yildirim, R. W. Li, J. H. Hung, P. B. Chen, X. J. Dong, L. S. Ee, Z. P. Weng, O. J. Rando and T. G. Fazzio, *Cell*, 2011, **147**, 1498-1510.

26 S. Kriaucionis and N. Heintz, *Science*, 2009, **324**, 929-930.

27 C. Ye and L. Li, *Cancer Bio. Ther.*, 2014, **15**, 10-15.

28 M. Valko, M. Izakovic, M. Mazur, C. J. Rhodes and J. Telser, *Mol. Cell. Biochem.*, 2004, **266**, 37-56.

29 M. J. Frisch, G. W. Trucks, H. B. Schlegel, G. E. Scuseria, M. A. Robb, J. R. Cheeseman, G. Scalmani, V. Barone, B. Mennucci, G. A. Petersson, H. Nakatsuji, M. Caricato, X. Li, H. P. Hratchian, A. F. Izmaylov, J. Bloino, G. J. Zheng, L. Sonnenberg, M. Hada, M. Ehara, K. Toyota, R. Fukuda, J. Hasegawa, M. Ishida, T. Nakajima, Y. Honda, O. Kitao, H. Nakai, T. Vreven, J. J. A. Montgomery, J. E. Peralta, F. Ogliaro, M. Bearpark, J. J. Heyd, E. Brothers, K. N. Kudin, V. N. Staroverov, R. Kobayashi, J. Normand, K. Raghavachari, A. Rendell, J. C. Burant, S. S. Iyengar, J. Tomasi, M. Cossi, N. Rega, J. M. Millam, M. Klene, J. E. Knox, J. B. Cross, V. Bakken, C. Adamo, J. Jaramillo, R. Gomperts, R. E. Stratmann, O. Yazyev, A. J. Austin, R. Cammi, C. Pomelli, J. W. Ochterski, R. L. Martin, K. Morokuma, V. G. Zakrzewski, G. A.Voth, P. Salvador, J. J. Dannenberg, S. Dapprich, A. D. Daniels, O. Farkas, J. B. Foresman, J.V. Ortiz, J. Cioslowski and D. J. Fox, *Gaussian 09*, Revision A.02. Gaussian, Inc., Wallingford, CT, 2009.

30 J. A. Montgomery, M. J. Frisch, J. W. Ochterski and G. A. Petersson, *J. Chem. Phys*., 1999, **110**, 2822-2827.

31 A. G. Baboul, L. A. Curtiss, P. C. Redfern and K. Raghavachari, *J. Chem. Phys*., 1999, **110**, 7650-7657.

32 B. Sirjean and R. Fournet, *J. Phys. Chem. A*, 2012, **116**, 6675-6684.

33 B. Sirjean, P. A. Glaude, M. F. Ruiz-Lòpez and R. Fournet, *J. Phys. Chem. A*, 2006, **110**, 12693-12704.

34 B. Sirjean, P. A. Glaude, M. F. Ruiz-Lòpez and R. Fournet, *J. Phys. Chem. A*, 2009, 113, 6924-6935.

35 J. W. Ochterski, G. A. Petersson and J. A. Montgomery, *J. Chem. Phys.* 1996, **104**, 2598-2619.

36 M. R. Nyden, G. A. Petersson, *J. Chem. Phys*., 1981, **75**, 1843-1862.

37 G. A. Petersson, A. Bennett, T. G. Tensfeldt, M. A. Al-Laham, W. Shirley and J. Mantzaris, *J. Chem. Phys.*, 1988, **89**, 2193-2218.

38 G. A. Petersson and M. A. Al-Laham, *J. Chem. Phys*., 1991, **94**, 6081-6090.

39 G. A. Petersson and M. Braunstein, *J. Chem. Phys*., 1985, **83**, 5105-5128.

40 J. A. Montgomery, J. W. Ochterski and G. A. Petersson, *J. Chem. Phys*., 1994, **101**, 5900-5909.

41 E. Cancès, B. Mennucci and J. Tomasi, *J. Chem. Phys*., 1997, **107**, 3032-3041.

42 W. J. Hehre, R. Ditchfield and J. A. Pople, *J. Chem. Phys.*, 1972, **56**, 2257-2261.

43 S. V. Jovanovic and M. G. Simic, *J. Am. Chem. Soc.*,1986, **108**, 5968-5972.

Table content:

Table 1 Relative energies [a] (kJ·mol^{-1}) for the reaction of •OH-mediated 5-hmCyt both in the gas and aqueous phases

Species	CBS-QB3[b]			PCM[c]	
	ΔE^g	ΔG^g	$\Delta G^{g\neq}$	ΔG^s	$\Delta G^{s\neq}$
		Addition Reactions			
R[d]	0.00	0.00		0.00	
IM1	-17.99	14.60		26.51	
TS1	-12.97	14.80		26.75	
P1	-83.74	-45.64		-38.21	
IM1	-17.99	14.60		26.51	
TS2	-15.33	20.41		31.65	
P2	-109.69	-73.94		-58.14	
IM1→P1			0.20		0.24
IM1→P2			5.81		5.14
		H-atom Abstraction Reactions			
IM3	-36.78	-2.48		11.11	
TS3	9.33	45.75		68.07	
P3	-32.08	2.22		-13.50	
IM4	-0.56	33.55		40.84	
TS4	6.96	43.53		60.55	
P4	-79.24	-45.12		-32.16	
IM5	-14.17	17.28		25.80	
TS5	-14.63	22.60		37.80	
P5	-162.60	-140.89		-139.62	
IM1	-17.99	14.60		26.51	
TS6	-3.06	30.20		31.25	
P6	-144.54	-130.66		-120.09	
IM1	-17.99	14.60		26.51	
TS7	17.44	50.87		65.03	
P7	-38.74	-14.05		-5.87	
IM8	-11.03	10.82		18.12	
TS8	13.80	46.93		62.98	
P8	-71.11	-37.09		-21.69	
IM3→P3			48.23		56.96
IM4→P4			9.98		19.71
IM5→P5			5.32		12.00
IM1→P6			15.60		4.74
IM1→P7			36.27		38.52
IM8→P8			36.11		44.86

[a] ΔE^g, ΔG^g, and $\Delta G^{g\neq}$ are relative energy, relative free energy, and activation free energy in the gas phase, respectively; ΔG^s and $\Delta G^{s\neq}$ are relative free energy and activation free energy with PCM model based on the optimized geometries in the aqueous phase. [b] CBS-QB3 composite approach. [c] CBS-QB3 with PCM model. [d] denotes 5-hmCyt+•OH.

Table 2 The partial atomic spin densities in the gas phase for the reactant complexes, transition states and products of •OH-mediated 5-hmCyt

Species	Reactant complexes							
	IM1		IM3	IM4	IM5	IM1		IM8
O1	0.75		1.03	0.81	1.03	0.75		0.99
N4				0.18				
C5	0.22					0.22		
C6	-0.01					-0.01		
	Transition states							
	TS1	TS2	TS3	TS4	TS5	TS6	TS7	TS8
O1	0.59	0.64	0.54	0.46	1.02	0.90	0.53	0.63
N3				0.20				
N4			0.45	0.43				
C5	0.03	0.36					0.03	
C6	0.26	-0.06					0.32	
O3								0.30
	Products							
	P1	P2	P3	P4	P5	P6	P7	P8
N1	0.10							
O1			0.11					
O2	0.13							
N3		0.25		0.33				
C4		-0.12		-0.16				
N4			0.86	0.76			0.87	
C5		0.79			-0.18	-0.18		0.13
C6	0.74				0.42	0.40		
C7					0.61	0.63		
O3								0.73

Table 3 The evolution of the dipole moments (μ, in debye) for the reactions of •OH-mediated 5-hmCyt (R1~R8)

R1	μ	R2	μ	R3	μ	R4	μ	R5	μ	R6	μ	R7	μ	R8	μ
IM1	5.68	IM1	5.68	IM3	8.73	IM4	4.07	IM5	5.95	IM1	5.68	IM1	5.68	IM8	8.31
TS1	5.84	TS2	5.89	TS3	8.30	TS4	4.00	TS5	5.24	TS6	6.28	TS7	5.72	TS8	5.36

Captions:

Fig. 1 Optimized structures (bond distances in Å) in the gas phase for the addition reaction of •OH mediated 5-hmCyt (paths R1 and R2) at the CBS-QB3 composite approach.

Fig. 2 The map of spin densities distribution for the reactant complexes, transition states and product radicals for the •OH addition to C5=C6 bond of 5-hmCyt and abstraction hydrogen (the H5 of C7 and H7 of cyclic C6 atoms) in the gas phase.

Fig. 3 Optimized structures (bond distances in Å) in the gas phase for the hydrogen-abstraction reaction (the H3 and H4 of NH_2 group) for •OH mediated 5-hmCyt (paths R3 and R4) at the CBS-QB3 composite approach.

Fig. 4 Optimized structures (bond distances in Å) in the gas phase for the hydrogen-abstraction reaction (the H5 and H6 of C7 atom) for •OH mediated 5-hmCyt (paths R5 and R6) at the CBS-QB3 composite approach.

Fig. 5 Optimized structures (bond distances in Å) in the gas phase for the hydrogen-abstraction reaction (the H7 of cyclic C6 and H8 of O3 atoms) for •OH mediated 5-hmCyt (paths R7 and R8) at the CBS-QB3 composite approach.

Fig. 6 The potential energy surfaces (ΔG^g in $kJ \cdot mol^{-1}$) along the reaction of •OH-mediated 5-hmCyt in the gas phase. R denotes 5-hmCyt +•OH. (a) is the addition reaction (paths R1 and R2), (b) is the hydrogen-abstraction reaction (paths R3-R8).

Fig. 7 The map of spin densities distribution for the reactant complexes, transition states and product radicals for the •OH abstraction hydrogen from 5-hmCyt (the H3 and H4 of NH_2 group, the H5 of C7 atom and the H8 of O3 atom) in the gas phase.

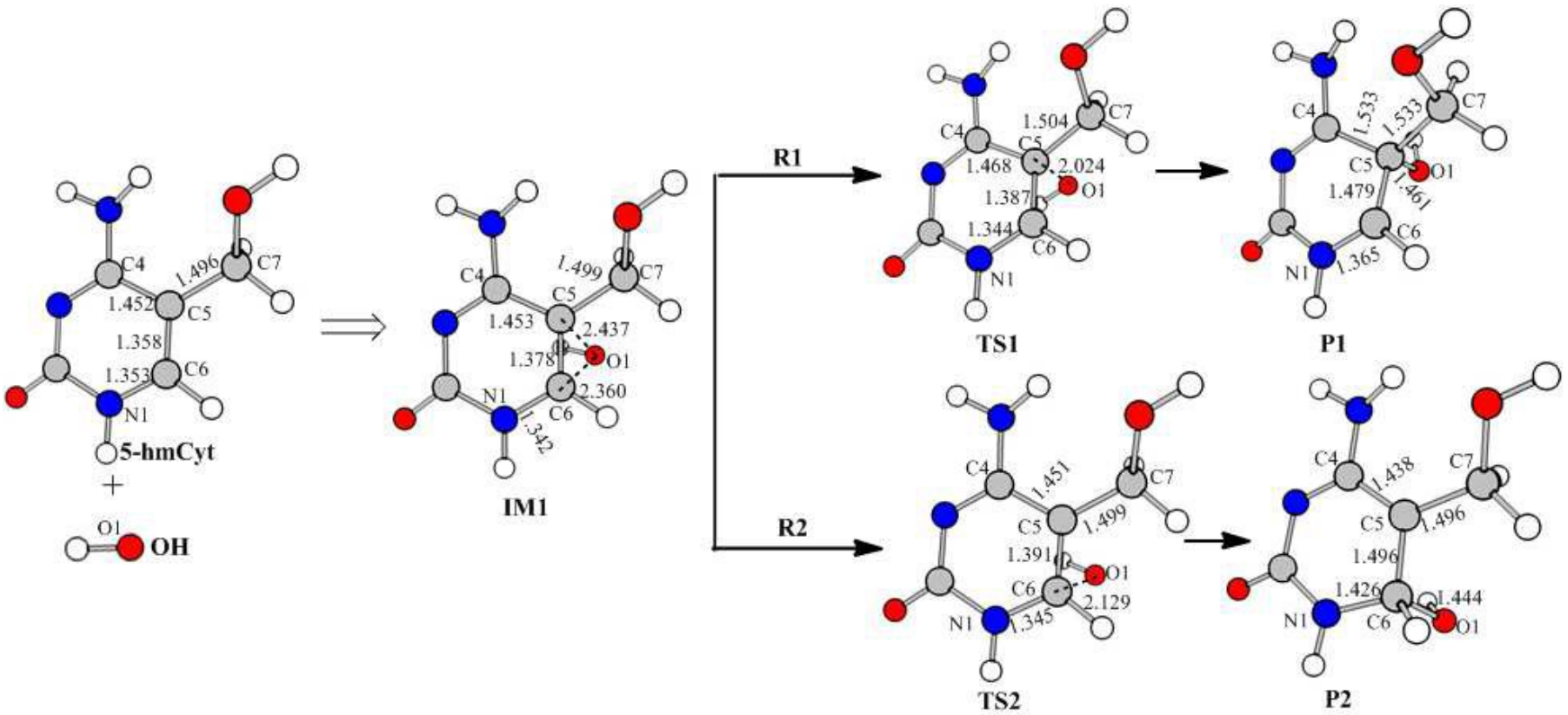

Fig.1

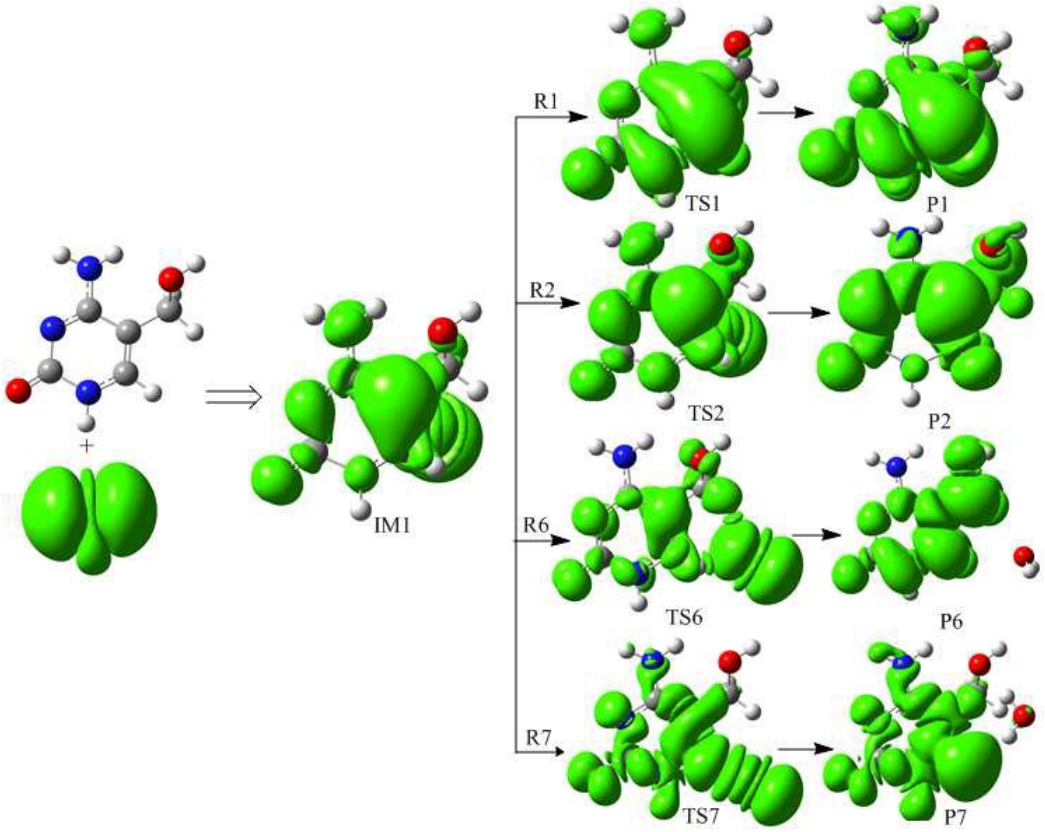

Fig.2

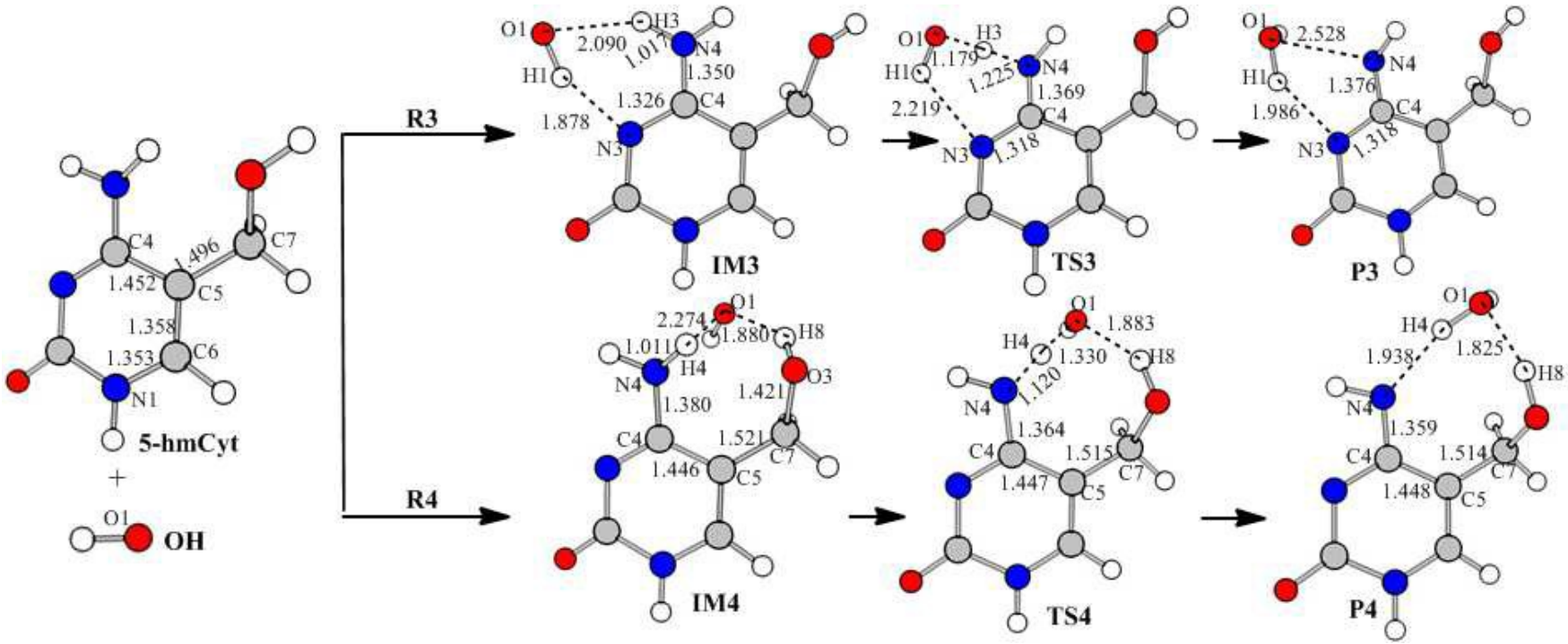

Fig.3

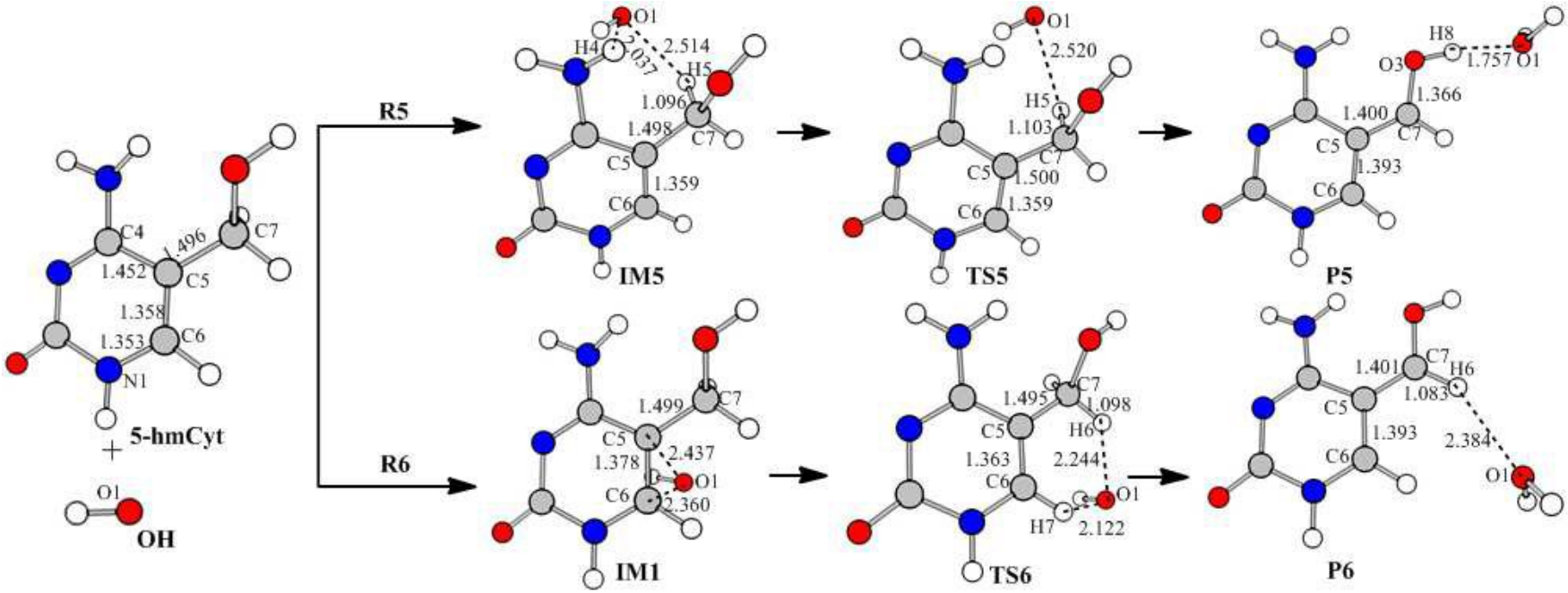

Fig.4

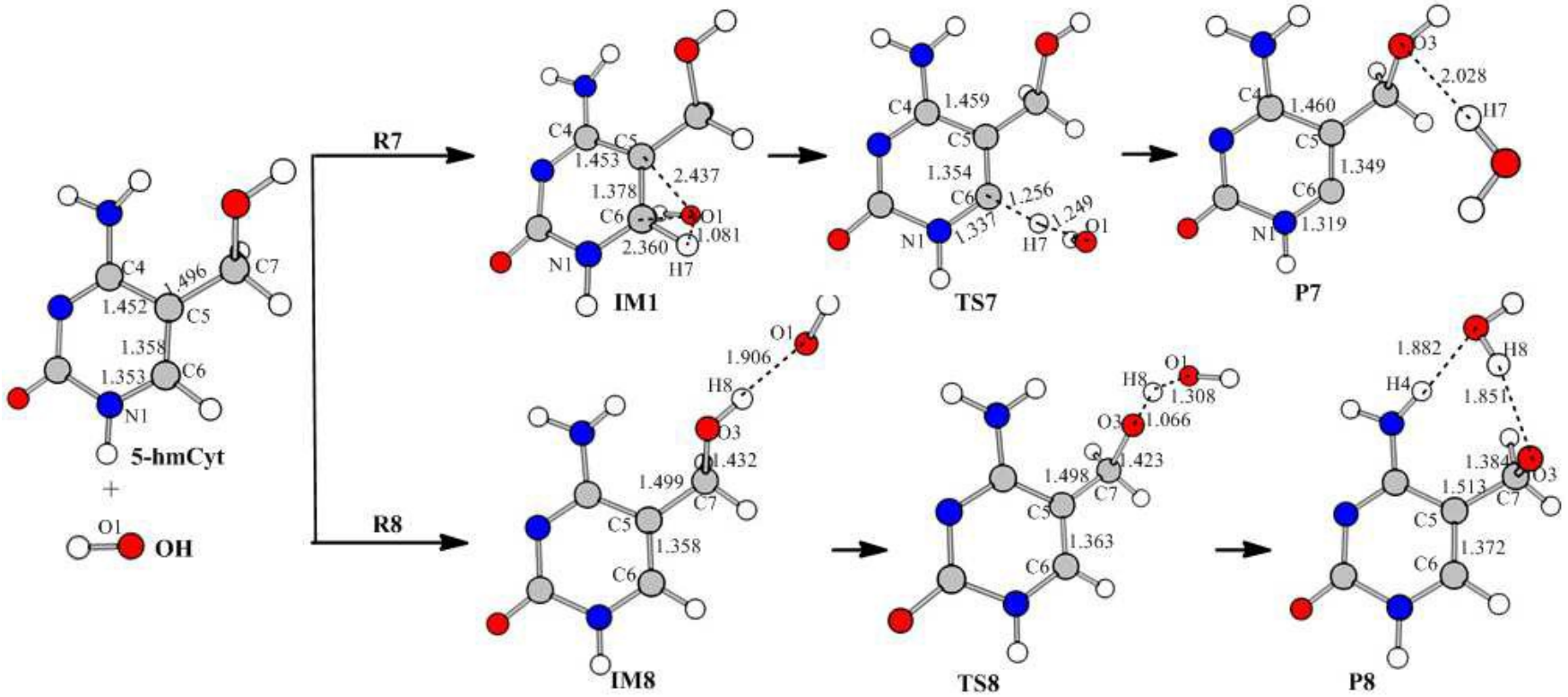

Fig.5

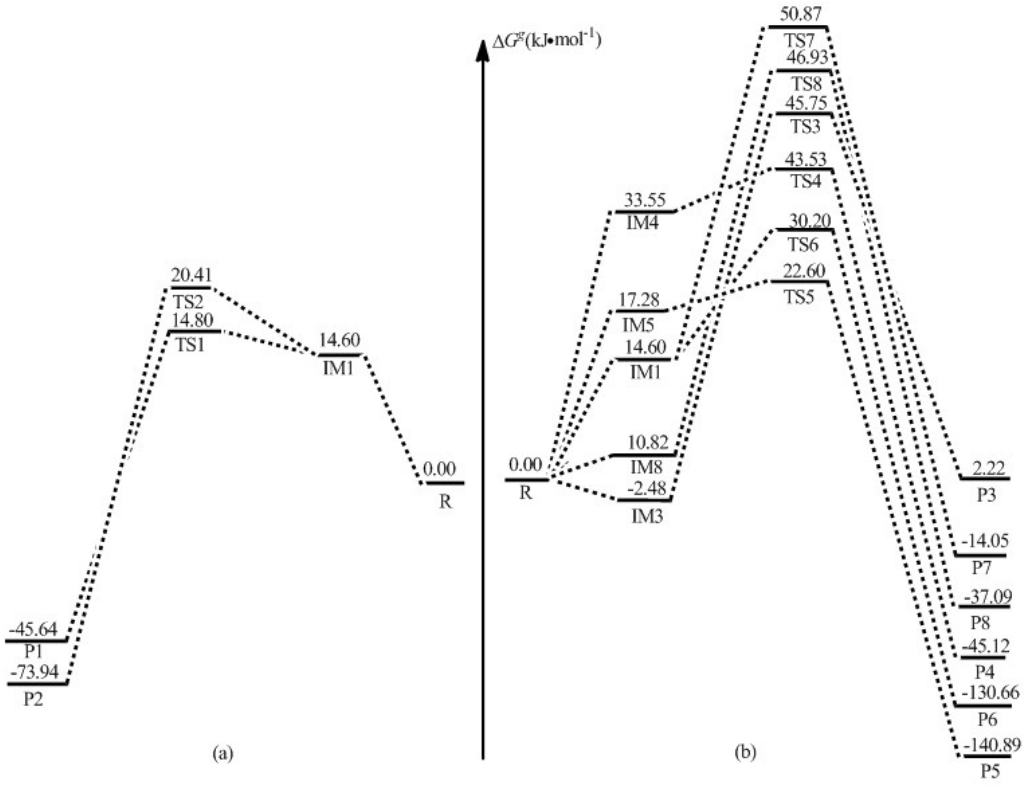

Fig.6

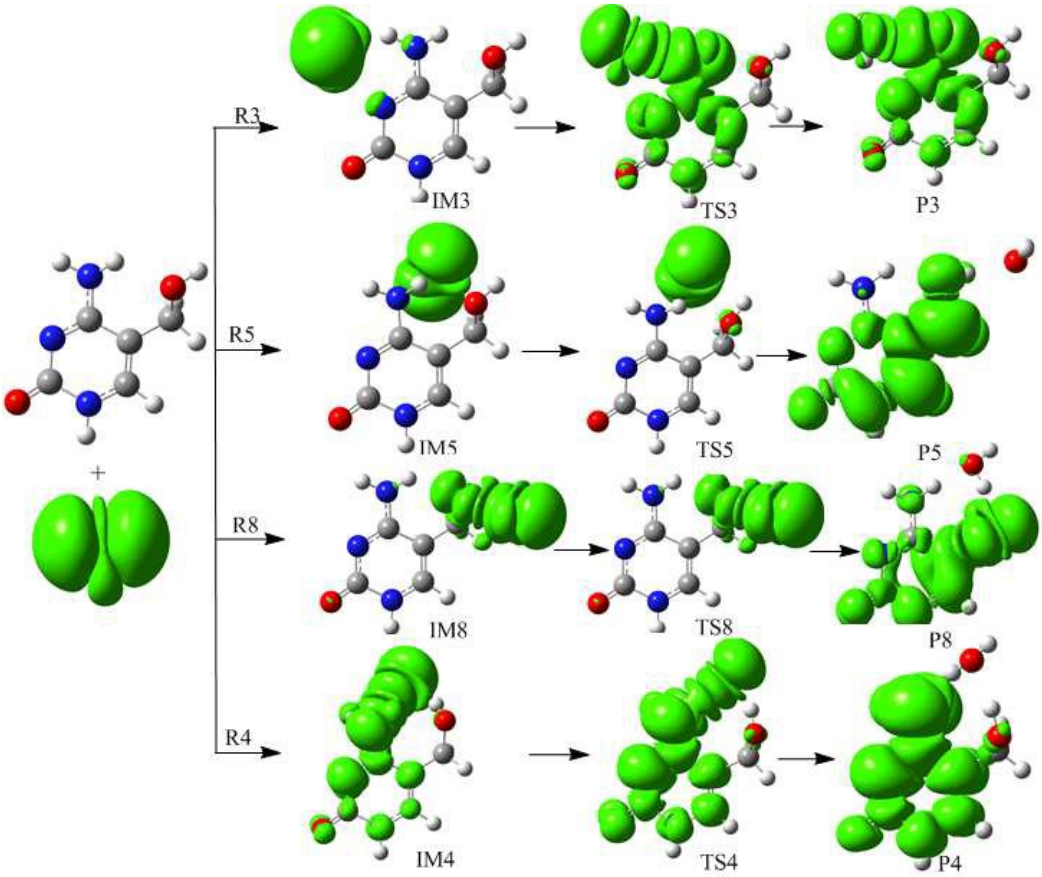

Fig.7

Graphical Abstract

The multi-channel reaction of OH radical with 5-hydroxymethylcytosine: a computational study

Lingxia Jin Caibin Zhao Cunfang Liu Suotian Min Tianlei Zhang Zhiyin Wang Wenliang Wang Qiang Zhang

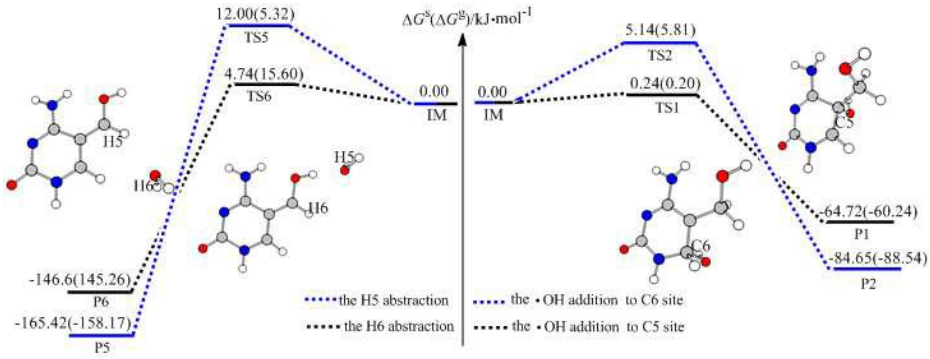

The solvent effects of water do not significantly alter the energetics of the addition and abstraction paths. The $\Delta G^{s\neq}$ value of C5 channel is a little lower than that of C6 route, indicating some amount of regioselectivity. The H5 and H6 abstraction reactions have almost the same energy barriers as those of •OH addition to C5 and C6 sites, leading to the formation of stable benzyl-radical-like complexes. This suggests the H5 and H6 dehydrogenation products may be detectable in experiments.